Journal of Energy Storage 72 (2023) 108199

Contents lists available at ScienceDirect

Journal of Energy Storage

journal homepage: www.elsevier.com/locate/est

Research papers

Optimization of an improved calcium-looping process for thermochemical energy storage in concentrating solar power plants

D. Rodrigues [a,b,c,d,e,*], C.I.C. Pinheiro [a,f], R.M. Filipe [b,g], L.F. Mendes [h,i], H.A. Matos [b,f]

[a] Centro de Química Estrutural, Institute of Molecular Sciences, Instituto Superior Técnico, Universidade de Lisboa, Av. Rovisco Pais 1, 1049-001 Lisboa, Portugal
[b] Centro de Recursos Naturais e Ambiente, Instituto Superior Técnico, Universidade de Lisboa, Av. Rovisco Pais 1, 1049-001 Lisboa, Portugal
[c] LSRE-LCM - Laboratory of Separation and Reaction Engineering – Laboratory of Catalysis and Materials, Faculdade de Engenharia, Universidade do Porto, Rua Dr. Roberto Frias, 4200-465 Porto, Portugal
[d] ALiCE - Associate Laboratory in Chemical Engineering, Faculdade de Engenharia, Universidade do Porto, Rua Dr. Roberto Frias, 4200-465 Porto, Portugal
[e] Departamento de Engenharia Química, Faculdade de Engenharia, Universidade do Porto, Rua Dr. Roberto Frias, 4200-465 Porto, Portugal
[f] Departamento de Engenharia Química, Instituto Superior Técnico, Universidade de Lisboa, Av. Rovisco Pais 1, 1049-001 Lisboa, Portugal
[g] Departamento de Engenharia Química, Instituto Superior de Engenharia de Lisboa, Instituto Politécnico de Lisboa, R. Conselheiro Emídio Navarro 1, 1959-007 Lisboa, Portugal
[h] IN+/LARSyS, Instituto Superior Técnico, Universidade de Lisboa, Av. Rovisco Pais 1, 1049-001 Lisboa, Portugal
[i] Departamento de Física, Instituto Superior Técnico, Universidade de Lisboa, Av. Rovisco Pais 1, 1049-001 Lisboa, Portugal

ARTICLE INFO

Keywords:
Concentrated solar energy
Thermochemical energy storage
Calcium looping
Process optimization
Process integration
Fluidization

ABSTRACT

The calcium-looping (CaL) process comprises an endothermic calcination reaction, where CaO and CO_2 are generated from $CaCO_3$, and its reverse exothermic carbonation reaction. CaL is promising for thermochemical energy storage (TCES) in concentrating solar power plants. The CaL-TCES process includes: a calciner where solar energy is transformed into thermochemical energy; a carbonator where the stored energy is released; turbines for electrical power generation; and tanks where the reaction products are stored. In this work, the CaL-TCES process is simulated and optimized using gPROMS Process. The innovation lies in identifying process improvements: make-up and purge streams to reduce CaO deactivation after cycling; a water separation process at the calciner outlet to allow calcination with water vapor as fluidizing gas; and the use of several degrees of freedom for process optimization. The goal is to maximize the thermal-to-electrical efficiency. By optimizing the carbonator and main turbine outlet pressures, the efficiency is improved from 38.1 % in the literature to 39.2 %. When make-up and purge streams are considered, the savings in power supply owing to the purged CaO allow improving the efficiency to 43.0 %. The water separation process reduces the thermal-to-electrical efficiency to 34.7 %, but allows a higher solar-to-thermal efficiency or a smaller calcination reactor.

1. Introduction

The variability of some types of renewable energy is considered one of the main obstacles to their widespread adoption. Energy storage is essential to deal with this issue. Concentrating solar power (CSP) systems rely on the concentration of solar energy in a receiver, allowing high-temperature thermal energy storage (TES) and power dispatchability. The most common solution for TES relies on nitrate-based molten salts as heat transfer and storage medium, the operational limitations of which do not allow high efficiencies since they need to be kept between 220 °C and 560 °C. An alternative method for TES in CSP systems is thermochemical energy storage (TCES), which is based on reversible reactions. For example, a promising option is the calcium-looping (CaL) process for TCES, which relies on a cycle that comprises (i) an endothermic calcination reaction, with a standard enthalpy of reaction of 178.4×10^3 J mol^{-1}, in which CaO and CO_2 are generated from $CaCO_3$ in a solar reactor, and (ii) an exothermic carbonation reaction, in which $CaCO_3$ is formed from CaO and CO_2. The reaction products are stored in tanks until the reverse reaction is carried out. This process is advantageous with respect to the use of molten salts since CaO precursors such as limestone are cheap, abundant, and harmless, the energy density is large (> 3 GJ m^{-3}), and carbonation can occur at high temperatures, which improves the efficiency in CSP plants [1]. A main disadvantage is CaO deactivation after several cycles, which decreases

* Corresponding author at: LSRE-LCM - Laboratory of Separation and Reaction Engineering – Laboratory of Catalysis and Materials, Faculdade de Engenharia, Universidade do Porto, Rua Dr. Roberto Frias, 4200-465 Porto, Portugal.
E-mail addresses: dfrodrigues@fe.up.pt, dfmr@tecnico.ulisboa.pt (D. Rodrigues), carla.pinheiro@tecnico.ulisboa.pt (C.I.C. Pinheiro), rfilipe@isel.ipl.pt (R.M. Filipe), filipe.mendes@tecnico.ulisboa.pt (L.F. Mendes), henrimatos@tecnico.ulisboa.pt (H.A. Matos).

https://doi.org/10.1016/j.est.2023.108199
Received 20 January 2023; Received in revised form 9 June 2023; Accepted 26 June 2023
Available online 20 July 2023

the conversion in the carbonator [2]. More details about the CaL-TCES process can be found in a recent review paper by Yan et al. [3].

Several versions of the CaL-TCES process have been proposed, which typically include a heat exchanger network around the calciner and the carbonator to promote heat integration and to increase the process efficiency. Edwards and Materić [4] proposed a first version of the CaL-TCES process, based on an open and direct Brayton cycle where air without CO_2 is used as the heat transfer fluid between the energy release in the carbonator and the gas turbine for power production and is then released to the environment. However, the assumption that air without CO_2 leaves the carbonator is not satisfied since the equilibrium pressure of CO_2 in a carbonation reaction is not zero. Chacartegui et al. [2] proposed a CaL-TCES process with a closed and direct CO_2 Brayton cycle, where CO_2 is fed to the carbonator in excess and the non-reacting CO_2 transfers the energy released in the carbonator to a gas turbine for electrical power generation. Alovisio et al. [5] showed that the heat exchanger network proposed by Chacartegui et al. [2] is the optimal one according to a pinch-analysis methodology. Ortiz et al. [6] concluded that a closed and direct CO_2 Brayton cycle allows achieving higher efficiencies than closed and indirect cycles, such as a steam Rankine cycle or a supercritical CO_2 Brayton cycle, or even a combined cycle with both the direct CO_2 Brayton cycle and the indirect steam Rankine cycle. According to these studies, process efficiencies of around 45 % can be achieved with the proposed cycle. However, continuous solid–solid heat exchangers and gas–solid heat exchangers with counter-current flow are assumed in these works, which may be unrealistic. For this reason, Ortiz et al. [7] proposed another version of the CaL-TCES process with a closed and direct CO_2 Brayton cycle and without these types of heat exchangers. Efficiencies above 38 % were achieved for specific carbonator and main turbine outlet pressures, but their combined effect was not fully evaluated. Pascual et al. [8] studied the performance of the CaL-TCES process for various combinations of storage and discharge modes regarding storage and heat exchangers, while Bailera et al. [9] focused on the sizing of the carbonator. However, heat integration was not considered. Ortiz et al. [10] proposed the integration of the CaL-TCES process in combined cycles to increase the solar power share of Integrated Solar Combined Cycles, while Ortiz et al. [11] applied this concept to deal with the variability of the solar power input throughout the day and the year. Both works consider the use of a heat transfer fluid such as CO_2 that passes through irradiated tubes in a solar receiver and transfers heat to the calciner via coiled heat exchangers when solar radiation is available, while similar coiled heat exchangers are used to transfer heat from the carbonator to the fluid when solar radiation is not available. However, solid–gas reactors driven by concentrated solar energy, in particular indirectly irradiated fluidized bed reactors, represent a viable technology with potential application to solar calcination in the CaL-TCES process [12], and other configurations of the CaL-TCES process do not require significant heat exchange in the carbonator [7]. In contrast, the configuration proposed by Ortiz et al. [10] and Ortiz et al. [11] hinders the role of radiation between an irradiated surface and a solid–gas suspension as an efficient heat transfer mechanism and requires very high receiver temperatures when solar radiation is available, while it also implies significant heat exchange in the carbonator, which may lead to large receiver losses and requires coupling the calcination and carbonation reactors to very large heat exchangers.

In the CaL process for post-combustion CO_2 capture, which has been thoroughly discussed in the literature, a make-up stream with fresh $CaCO_3$ is typically added to the calciner and a purge stream is used to remove the spent sorbent and to prevent excessive CaO deactivation [13]. The deactivated CaO in the purge stream can then be used as a raw material for cement production [14]. However, the previous studies found in the literature about the CaL-TCES process do not consider $CaCO_3$/CaO make-up and purge streams, which would also enable efficiency gains in the CaL-TCES process owing to the conversion of $CaCO_3$ to CaO.

In several works related to the CaL process for post-combustion CO_2 capture, fluidized bed reactors have been used for calcination [15]. Since it is expected that these reactors would also be used for calcination in the CaL process for TCES, computational models of these reactors have been developed by Lisbona et al. [16] and Rodrigues et al. [17]. The CaL-TCES process described in the literature implicitly assumes that the gas phase in the calciner contains pure CO_2 since no gas separation unit or process is included. However, in fact, it would be beneficial to use another gas for fluidization since it would increase the reaction rate and would make the calcination reaction more thermodynamically favorable owing to a lower equilibrium temperature. In turn, this would enable the use of a smaller residence time and a lower temperature in the calciner, and consequently, a smaller reactor and a reduction of the radiative energy losses. Water vapor in a mixture with the CO_2 generated by the calcination reaction is a particularly suitable option as a fluidizing gas for calcination since it is abundant and commonly used in the industry and can be separated from CO_2 via condensation at moderate pressures and temperatures. However, the literature simply mentions the existence of an energy penalty associated with the use of water vapor for calcination in the CaL-TCES process due to the energy consumption to bring back the water vapor to the calcination temperature after separation, without quantifying that penalty [1]. Hence, it would be useful to develop a process for water separation that minimizes energy consumption and to quantify that energy consumption.

The effect of the presence of water vapor during calcination or carbonation on the reactivity and cyclic behavior of $CaCO_3$/CaO for the CaL process has been studied, both for post-combustion CO_2 capture and for TCES.

The following results were obtained in the conditions of CaL-CO_2 capture: (1) The conversion of about 70 % of carbonation of the CaO produced with H_2O during calcination is higher than the conversion of about 40 % of the CaO produced in 100 % CO_2 [18]. (2) The carrying capacity after 10 cycles is significantly improved with H_2O during calcination (up to 30 %) with respect to the case without H_2O (between 11 % and 19 %). The improvement was observed even with only 0.1 % H_2O, while no significant improvement was obtained from 1 % to 20 % H_2O, and a synergy was observed when H_2O is present for both calcination and carbonation [19]. (3) Water during calcination has a positive effect on the carrying capacity of CaO and on the carbonation reaction rate, with the optimal performance at 15 % H_2O. On the other hand, 40 % H_2O combined with a lower calcination temperature of 875 °C allows achieving the highest carrying capacity, and H_2O during carbonation improves the carrying capacity more than H_2O during calcination [20]. (4) A synergy was observed between doping with bromides and the presence of H_2O, which increases the CO_2 uptake to 37 g/100 g of sorbent after 10 cycles from the uptake of 14 g/100 g of sorbent for undoped sorbent and no H_2O present. Also, the uptake after 5 min is 4 times higher for doped pellets in the presence of H_2O [21]. (5) A higher content of impurities leads to a larger reduction of the calcination reaction time caused by the presence of H_2O. [22].

The following results were obtained in the conditions of CaL-TCES: (1) Water at 3 % and 29 % during calcination increases the reaction rate and allows full calcination at 700 °C in less than 10 min, and 29 % H_2O allows decreasing the calcination temperature to 680 °C and increases the multicycle performance by about 50 %. The activation energy of carbonation is reduced from 175 kJ/mol for calcination without H_2O to 142 kJ/mol for calcination at 29 % H_2O [23]. (2) Water during carbonation does not affect the residual conversion, although the use of N_2/CO_2 improves the residual conversion with respect to 100 % CO_2. This contrasts with CaL-CO_2 capture, where H_2O during both calcination and carbonation improves the multicycle performance of CaO [24]. (3) The conversion of the carbonation reaction is lower when calcination is performed with H_2O at 3 % and 29 % in CO_2 than when H_2O at 3 % and 29 % in N_2 is used and increases more with the concentration of H_2O in the latter case, although just 3 % H_2O

in CO_2 already results in substantial improvement of the multicycle performance. Water during calcination also allows using larger particles with more than 100 μm with improved multicycle performance [25]. (4) The calcination temperature in the presence of H_2O is lower than when dry N_2 is used. The calcination kinetics can be described by a single rate expression that includes the effect of temperature and H_2O partial pressure by using parameters such as the exponent (around 0.14) of a power of the H_2O partial pressure that expresses its acceleration effect [26]. (5) The multicycle conversion of CaO calcined under H_2O is slightly lower than under N_2, but more than 5 times larger than under pure CO_2, while calcination under H_2O occurs at a lower temperature and faster rate than under N_2. Although calcination at 100 % H_2O aggravates the attrition of limestone, an 80 % H_2O mixture in CO_2 does not affect much the heat storage performance and the calcination temperature and reaction rate, while it improves the attrition resistance [27].

However, as the literature review about the effect of water vapor in the previous paragraphs shows, most of this literature concerns: (i) the CaL-CO_2 capture process, which uses operating conditions that are rather different from the ones that are used in the CaL-TCES process; or (ii) experimental studies about the effect of the presence of water vapor during calcination and/or carbonation on the properties of the $CaCO_3$/CaO mixture, which do not directly deal with the implementation of the use of water vapor as fluidizing gas in the solar calciner of the CaL-TCES process and its implications. In contrast, the current paper (i) shows how the use of water vapor during calcination could be implemented in the CaL-TCES process via a water separation process at the calciner outlet, (ii) proposes a specific process to implement this water separation, and (iii) quantifies the effect of this water separation process on the thermal-to-electrical efficiency of the whole CaL-TCES process.

In this work, three innovative aspects with respect to the literature are introduced: (i) the CaL-TCES process is optimized by choosing optimal values of key variables such as the carbonator and main turbine outlet pressures; (ii) the existence of make-up and purge streams is considered, and their effect on the efficiency gains owing to the conversion of $CaCO_3$ to CaO is evaluated; (iii) a process for water separation from the gas stream at the outlet of the solar calciner is proposed, with the goal of enabling the use of water vapor for fluidization in the calciner and quantifying the associated energy penalty. The CaL-TCES process proposed by Ortiz et al. [7], for which a basic flowchart is shown in Fig. 1, is used as a benchmark and starting point for a simulation and optimization study of a process with optimized operating conditions. To this end, the maximization of the thermal-to-electrical efficiency subject to relevant process constraints is formulated as an optimization problem. To the best of our knowledge, this work proposes the use of numerical methods for optimization of the CaL-TCES process for the first time. Although other relevant aspects related to process design and operation are mentioned as a motivation for the modeling choices, this work focuses on the quantification and optimization of the thermal-to-electrical efficiency.

2. Process modeling and optimization

As mentioned, the CaL-TCES process that is simulated and optimized in this work is based on the process proposed by Ortiz et al. [7]. The current work also includes the simulation and optimization of a water separation process to allow using water vapor as fluidizing gas in the solar calciner.

2.1. Description of the CaL-TCES process

Figs. 2 and 3 show a simplified schematic of the CaL-TCES process when solar radiation is available or not. The process includes: a solar calciner (CALC) at 900 °C and 1 bar where solar energy heats up a mixture of $CaCO_3$ and CaO and fully converts $CaCO_3$ to CaO and CO_2; a carbonator (CARB) at 850 °C where the chemically stored energy is released by converting CaO and CO_2 to $CaCO_3$; turbines for electrical power generation; tanks modeled as sources and sinks, where the reaction products are stored before their use as reactants; and a heat exchanger network around the reactors to enable heat integration.

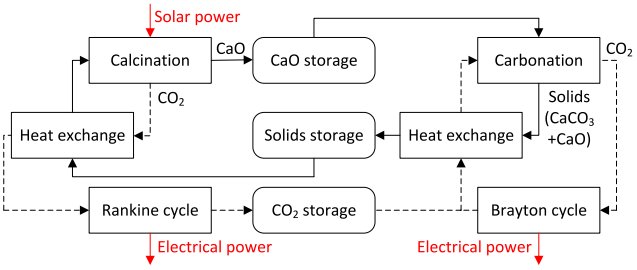

Fig. 1. Basic flowchart of the CaL-TCES process proposed by Ortiz et al. [7]. Black solid lines represent material flow of solid streams, black dashed lines represent material flow of gas streams, and red lines represent energy flow.

When solar radiation is available, calcination occurs in the solar calciner, and the CO_2 that leaves the calciner (i) heats up the solids that enter the calciner in a cyclone modeled as a co-current heat exchanger (GSHE1) and (ii) evaporates water in a heat recovery steam generator (HRSG) that provides steam at 400 °C and 40 bar, which is then used in a Rankine cycle with a steam turbine (ST), a condenser (COND) at 0.075 bar, and a pump (P1); a part of the CO_2 passes through a high-pressure compressor (HCOMP) before entering the CO_2 storage tank at 25 °C and 75 bar when solar radiation is available and passes through a high-pressure gas turbine (HTURB) after leaving the storage tank when no solar radiation is available. The CO_2 that enters the carbonator either (i) passes through the main compressor (MCOMP) or (ii) comes from the calciner after passing through the auxiliary compressor (MCOMD) when solar radiation is available or from the CO_2 storage tank when no solar radiation is available; a fraction (determined by a splitter) of this CO_2 is pre-heated by the CO_2 that leaves the carbonator and passes through the main gas turbine (MTURB) in a gas–gas heat exchanger (HXG); the remaining CO_2 that enters the carbonator is pre-heated in a cyclone (GSHE2) by solids; these solids are the ones that leave the carbonator and are then used in another cyclone (GSHE3) to heat up all the CO_2 just before it enters the carbonator. The process on the carbonator side operates continuously for 24 h every day, while the process on the calciner side operates only when solar radiation is available. The implementation details in gPROMS Process are given in Section S1 (Supplementary Material).

2.2. Description of the water separation process

As previously mentioned, the CaL-TCES process described in the literature implicitly assumes that the gas phase in the calciner is composed of pure CO_2. In this paper, this assumption is eliminated by using a fluidizing gas for the calcination reactor that consists of water vapor in a mixture with the CO_2 generated by the calcination reaction. Section S2 justifies why this use of water vapor decreases the thermal losses, reduces CaO deactivation, and allows the use of a smaller residence time. This is enabled by a process that is proposed for water separation from the CO_2 in the gas stream at the calciner outlet. This subsection focuses on this water separation process.

The goal is to propose a process for separation of the gas outlet stream of the solar calcination reactor, which includes the water vapor used for fluidization in the calcination reactor as well as the CO_2 generated by the calcination reaction, into two streams: (i) one with a high fraction of water to be recycled to the inlet of the calcination reactor; and (ii) another with a high fraction of CO_2 to replace the gas outlet stream of the calcination reactor for the case of calcination under pure CO_2. At the same time, the separation process should ensure

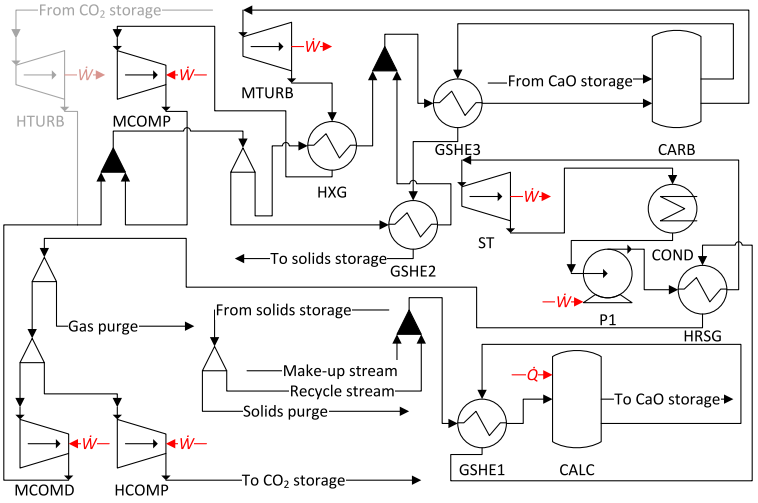

Fig. 2. Schematic of the CaL-TCES process when solar radiation is available. Legend: $\dot{Q}$ — Solar power; $\dot{W}$ — Electrical power; CALC — Calciner; CARB — Carbonator; COND — Condenser; GSHE — Gas–solid heat exchanger; HCOMP — High-pressure compressor; HRSG — Heat recovery steam generator; HXG — Gas–gas heat exchanger; MCOMD — Auxiliary compressor; MCOMP — Main compressor; MTURB — Main gas turbine; P — Pump; ST — Steam turbine. Light shading represents equipment that is not operating, filled triangles represent mixers, and triangles without filling represent splitters.

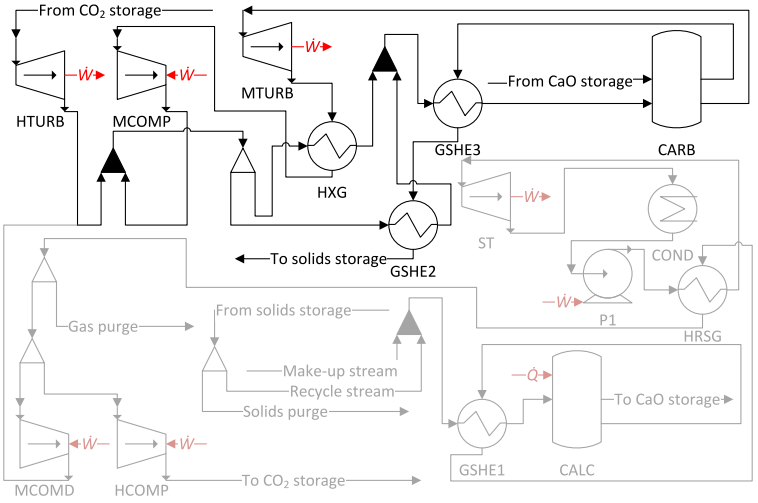

Fig. 3. Schematic of the CaL-TCES process when solar radiation is not available. Legend: $\dot{Q}$ — Solar power; $\dot{W}$ — Electrical power; CARB — Carbonator; COND — Condenser; GSHE — Gas–solid heat exchanger; HTURB — High-pressure gas turbine; HXG — Gas–gas heat exchanger; MCOMP — Main compressor; MTURB — Main gas turbine. Light shading represents equipment that is not operating, filled triangles represent mixers, and triangles without filling represent splitters.

that its two outlet streams reach the same temperature of 900 °C and pressure of $p_0 = 1$ bar of the gas outlet stream that leaves the calcination reactor, while avoiding as much as possible the consumption of any thermal energy for this separation. As described below, almost all the energy consumption in this separation process is related to the use of compressors to recompress the water vapor to the pressure p_0, which, along with the proposed order of unit operations, allows avoiding as much as possible consumption of any thermal energy for separating and restoring the same conditions of the gas outlet stream of the solar calcination reactor.

The proposed process for separation of water and CO_2 at the calciner outlet includes: n stages of unit operations; and an initial cooling step and a final separation and heating step for the streams before and after the separation stages. This is shown by the basic flowchart in Fig. 4, which does not include heat integration for the sake of simplicity. The main idea in this process is to enable heat integration between condensation/cooling and evaporation/heating in each basic separation stage and between the initial cooling and final heating steps before and after the separation stages. In particular, evaporation takes place before compression because this allows performing evaporation at a lower temperature, which is required to ensure that evaporation is performed at a lower temperature than condensation in each separation stage i since condensation occurs at pressure p_0. Hence, the basic separation stage i with heat integration is described by the simplified schematic in Fig. 5 and the initial and final steps with heat integration are described by the simplified schematic in Fig. 6. The number n of separation stages should be such that the fraction of water in the CO_2-rich vapor phase that leaves stage n is sufficiently small for the final separation step. The implementation details in gPROMS Process are given in Section S3. In particular, a value of $n = 3$ is used for this implementation. The stage i is characterized by a temperature T_i and a pressure p_i and is composed of several unit operations, as follows:

- The mixture of water and CO_2 that enters the stage for separation is divided into a vapor stream and a liquid stream according to the vapor–liquid equilibrium of water and CO_2 at pressure p_0 and temperature T_i in an adiabatic flash drum FLASHi.
- The vapor stream that leaves FLASHi as saturated vapor flows to the next stage $i + 1$ for separation, or to a final flash drum FLASH$(n + 1)$ for further separation if $i = n$.

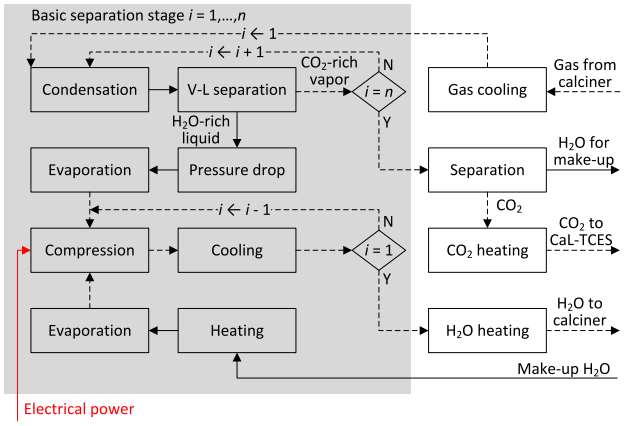

Fig. 4. Basic flowchart of the proposed water separation process without heat integration. Black solid lines represent material flow of liquid streams, black dashed lines represent material flow of gas streams, and red lines represent energy flow. (For interpretation of the references to color in this figure legend, the reader is referred to the web version of this article.)

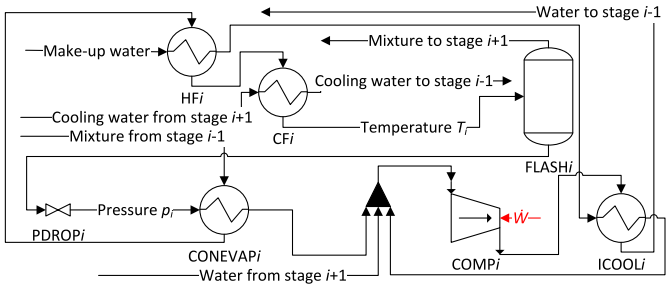

Fig. 5. Schematic of the separation stage i with heat integration in the water separation process. Legend: $\dot{W}$ — Electrical power; CF — Pre-flash cooler; COMP — Compressor; CONEVAP — Condenser/evaporator; FLASH — Flash drum; HF — Make-up water heater/pre-flash cooler; ICOOL — Intercooler; PDROP — Pressure drop. Filled triangles represent mixers.

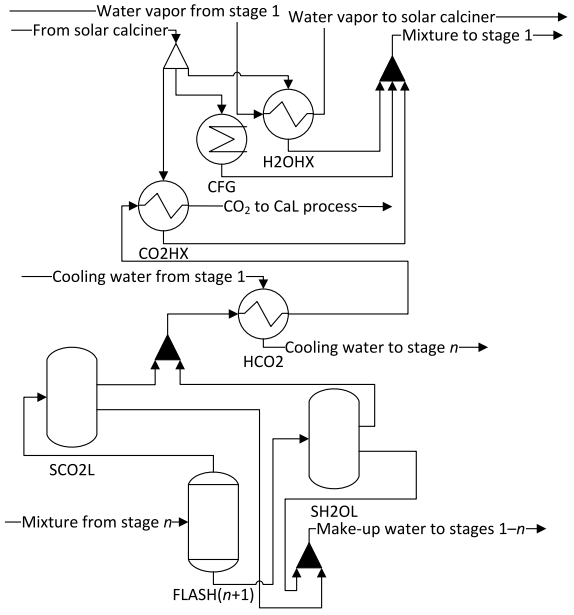

Fig. 6. Schematic of the initial cooling and final separation and heating steps with heat integration in the water separation process before and after the n separation stages. Legend: CFG — Cooler for fluidizing gas; CO2HX/H2OHX — Heat exchanger for initial cooling and final heating of CO_2/H_2O; FLASH — Flash drum; HCO2 — CO_2 heater; SCO2L/SH2OL — Low-temperature separator for CO_2/H_2O. Filled triangles represent mixers, and triangles without filling represent splitters.

- The liquid stream that leaves FLASHi as saturated liquid is subject to an adiabatic pressure drop from a pressure of p_0 to p_i in PDROPi.
- The gaseous mixture of water and CO_2 to be separated in the stage enters the heat exchanger CONEVAPi as vapor at pressure p_0 from the flash drum FLASH$(i-1)$ in the previous stage or, if $i = 1$, from the gas outlet stream of the calcination reactor after cooling. This mixture is the hot fluid and partially condensates by exchanging heat with a cold fluid that corresponds to the outlet stream of PDROPi, which leaves the heat exchanger as saturated vapor.
- To compensate for the water vapor that flows to the final flash drum and is not directly recovered from the liquid streams that leave the flash drums in the different stages, liquid make-up water at 40 °C is fed to each stage. The make-up water stream is heated up in the heat exchanger HFi by the hot outlet of CONEVAPi.
- The heat exchanger CFi is used to reduce the temperature of the hot outlet of HFi to T_i. It uses a stream of pure water as cooling fluid, where this stream comes from the corresponding heat exchanger HF$(i+1)$ in the next stage (or is at 40 °C if $i = n$) and goes to the corresponding heat exchanger HF$(i-1)$ in the previous stage (or to serve as hot fluid in the final heating step if $i = 1$).
- The stream that is evaporated in CONEVAPi, the make-up water stream that is evaporated as mentioned next, and the corresponding streams from the next stages enter a mixer as water-rich saturated vapor at pressure p_i. The resulting stream goes through the compressor COMPi, where its pressure is increased from p_i to p_{i-1}.
- Before the outlet stream of COMPi flows to the previous stage for further compression or to the final heating step if $i = 1$, it is used as hot fluid in the heat exchanger ICOOLi to evaporate the make-up water stream that corresponds to the cold outlet stream of HFi. This hot outlet stream becomes one of the inlet streams of the mixer in the previous stage for further compression or flows to the final heating step if $i = 1$.

The pressure ratios in the compressors COMPi in stages $i = 2, \ldots, n$ are the only available degrees of freedom in the separation process. The pressure ratio in the compressor COMP1 in stage 1 cannot be arbitrarily chosen since its outlet pressure must be equal to p_0.

Consequently, three streams flow out of the separation stages:

(1) A stream of CO_2-rich saturated vapor at pressure p_0, which leaves the flash drum FLASHn in stage n.
(2) A stream of water-rich saturated vapor at pressure p_0, which leaves the heat exchanger ICOOL1 in stage 1.
(3) A stream of pure water used as cooling fluid in the separation stages, which leaves the heat exchanger CF1 in stage 1.

The CO_2-rich stream in (1) is fed to a final flash drum at 40 °C to separate as much water as possible from the vapor stream. Then, the resulting vapor and liquid streams flow to the separators SCO2L and SH2OL, respectively. The water and the CO_2 that leave these separators are combined in corresponding mixers. The outlet stream of the CO_2 mixer is heated up in the heat exchanger HCO2, where the hot fluid corresponds to the water stream (3). The cold outlet stream of HCO2 and the stream (2) of water-rich saturated vapor are then subject to the final heating step.

As the final step of the water separation process, the two resulting streams need to be heated up to the temperature of 900 °C of the mixture of water and CO_2 that leaves the calciner. This is needed so that the water can be recycled to the calciner and the CO_2 can be used for solids preheating and steam generation in a Rankine cycle. To this end, the stream (2) of water-rich saturated vapor is heated up in the heat exchanger H2OHX, while the cold outlet stream of HCO2 is heated up in the heat exchanger CO2HX. In both cases, the gas outlet stream of the calcination reactor at 900 °C and 1 bar is used as the hot fluid. For this

reason, the two streams also pass through the heaters QH2O and QCO2 to increase their temperature to 900 °C, which are not represented in Fig. 6 since they may not be real heaters in the process, and this thermal power may be supplied by direct absorption of solar thermal energy in the solar calcination reactor.

In the stream of water-rich vapor, a small amount of CO_2 is still present, which is also recycled to the inlet of the calcination reactor. For this reason, it is also present in the gas outlet stream of the calcination reactor. The resulting gas stream at 900 °C and 1 bar enters the initial cooling and final heating step of the water separation process and is split into three streams: (1) the first one is the hot fluid in the heat exchanger H2OHX; (2) the second one is the hot fluid in the heat exchanger CO2HX; (3) the remaining hot fluid is cooled down in the cooler CFG. These three streams are then combined in a mixer, the outlet stream of which corresponds to the hot inlet stream of the heat exchanger CONEVAP1 in the separation stage 1.

2.3. Optimization procedure

The optimization goal of this study is the maximization of the thermal-to-electrical efficiency of the CaL-TCES process subject to the constraints mentioned in Sections 2.1 and S1. As a result, a nonlinear program (NLP) is obtained, the numerical solution of which is attained in an efficient way and allows achieving improved process efficiency. Thermal power is the heat supplied in the calciner, while electrical power is the difference between power generation in turbines and power consumption in pumps, compressors, coolers, and solids transport. Although previous studies have also aimed to achieve high thermal-to-electrical efficiency of the CaL-TCES process, the current study aims to maximize this efficiency via numerical optimization of an improved process. The following three points summarize the current situation and the possible improvements that have been identified in the literature, namely, in the work by Ortiz et al. [7] that is used as a benchmark and starting point for simulation and optimization of the CaL-TCES process:

(1) The two most relevant cases proposed by Ortiz et al. [7] are: a main turbine outlet pressure at 1 bar and a pressure ratio between the carbonator and main turbine outlet pressures varying around the nominal value of 3; and a carbonator outlet pressure at 1 bar and the same pressure ratio varying around the nominal value of 3. The nominal version of these two cases leads to efficiencies of 38.1 %, while an efficiency of 38.7 % is achieved by increasing the pressure ratio in the first case. However, both pressures can be modified independently, while only one pressure is changed at a time in the previous study.

(2) In the study by Ortiz et al. [7], the conversion in the carbonator is a parameter with a nominal value of 15 %, and a sensitivity analysis with respect to this parameter is performed. From this analysis, it is possible to conclude that a larger conversion leads to higher efficiency (38.7 % of efficiency is obtained for a conversion of 40 %). The process by Ortiz et al. [7] does not include make-up and purge streams, and it is implicitly assumed that the conversion in the carbonator corresponds to the residual conversion of CaO after many cycles, which is lower than the conversion for a small number of cycles. However, the residual conversion of CaO is determined by the sorbent used for the CaL-TCES process, and a residual conversion of 15 % or even lower is expected for typical limestone-based sorbents. As it is typically considered in the CaL-CO_2 capture process, this conversion may be increased by including make-up and purge streams in the process [28].

(3) The study by Ortiz et al. [7] implicitly assumes the use of pure CO_2 as the fluidizing gas in the solar calcination reactor since no separation process is used at the gas outlet of the calcination reactor. The use of water vapor as the fluidizing gas in the solar calcination reactor would be a way to reduce the calcination temperature and residence time. However, a process for water separation from the gas outlet stream of the calcination reactor has not been proposed and the resulting efficiency penalty has not been quantified in the literature.

The innovative procedure in this work addresses the three previous points and differs from the one by Ortiz et al. [7] in three relevant ways:

(1) The carbonator and main turbine outlet pressures are decision variables determined via numerical optimization.

(2) The presence of make-up and purge allows accounting for the energy savings owing to the CaO that leaves the process, which avoids the energy consumption for calcination of $CaCO_3$ in cement production plants. In this work, (i) make-up and purge streams are included, (ii) the conversion in the carbonator is computed according to the number of cycles experienced by the particles, which depends on the ratio between make-up and recycle molar flow rates, and (iii) the CaO that leaves the process through the solids purge stream is considered for the efficiency. In the proposed CaL-TCES process in Sections 2.1 and S1, a make-up stream (FRESH) with 100 % of fresh $CaCO_3$ is added to the recycle stream. The latter stream corresponds to the solids from the storage tank of carbonation products that do not leave the process in the solids purge stream (SPURGE), in contrast to some CaL processes for CO_2 capture, where the purge stream is located at the calciner outlet [28]. This location of the purge stream is required to avoid the situation where solar energy would be transformed into thermochemical energy in the calciner by forming CaO that would then be immediately released from the process, without taking advantage of the energy stored in CaO for conversion to electrical energy, which is the purpose of the CaL-TCES process. The heat duty required to cool down SPURGE to 40 °C is fully used to heat up FRESH from its initial temperature of 40 °C, although this solid–solid heat exchange does not need to be continuous. In addition, a CO_2 purge stream (GPURGE) is included after HRSG, and the molar flow rate of GPURGE is equal to the molar flow rate of CaO in SPURGE, while the molar flow rate of FRESH is equal to the molar flow rate of both $CaCO_3$ and CaO in SPURGE to ensure that the mass balance is satisfied. The split fraction of solids from the storage tank of carbonation products that leaves the process in SPURGE is considered as a decision variable.

(3) A process for water separation from the gas outlet stream of the calcination reactor is proposed, as shown in Section 2.2, and its effect on the thermal-to-electrical efficiency is quantified. In addition, as mentioned in Section 2.2, the pressure ratios in the compressors COMPi in stages $i = 2, \ldots, n$ are available as degrees of freedom. Hence, they are treated as decision variables and are determined via optimization such that the power consumption in the compressors COMPi is minimized.

2.4. Efficiency computation

More details are given below regarding how the conversion in the carbonator and the efficiency are computed. The fraction r_N of particles that have experienced N cycles in the carbonator is given by [29]

$$r_N = \frac{F_0 F_R^{N-1}}{\left(F_0 + F_R\right)^N}, \tag{1}$$

where F_0 is the make-up molar flow rate of FRESH or the solids purge molar flow rate of SPURGE and F_R is the recycle molar flow rate between SPURGE and FRESH, which implies that $F_0 + F_R$ is the inlet molar flow rate in CALC, labeled as the solids molar flow rate in the

remainder. The conversion of the particles that have experienced N cycles in the carbonator is [28]

$$X_N = \left(1 - X_r\right) k^N + X_r, \tag{2}$$

where $k = 0.77$ according to Abanades et al. [28] and $X_r = 0.15$ for consistency with the study by Ortiz et al. [7]. Then, the average conversion X_{ave} in the carbonator is given by [29]

$$X_{ave} = \sum_{N=1}^{\infty} r_N X_N. \tag{3}$$

By combining the previous equations, the analytical expression for the average conversion in the carbonator is

$$X_{ave} = \frac{\left(1 - X_r\right) k F_0}{F_0 + (1-k) F_R} + X_r = \frac{\left(1 - X_r\right) k f_p}{f_p + (1-k)\left(1 - f_p\right)} + X_r, \tag{4}$$

which is an explicit function of the solids purge split fraction f_p from the storage tank of carbonation products that leaves the process in SPURGE, where f_p is defined as

$$f_p = \frac{F_0}{F_0 + F_R} \tag{5}$$

and considered as a decision variable.

In this study, the efficiency depends not only on the generation and consumption of electrical power, but also on the power savings owing to the CaO that leaves the process in SPURGE. It is known that, from the perspective of cement production plants, for each mole of CaO in SPURGE that replaces a mole of $CaCO_3$ in FRESH, one can avoid the supply of high-temperature thermal energy that would be required for calcination of one mole of $CaCO_3$, which would be enabled by a burner with an efficiency η_b. Since that consumption is avoided, electrical power can be produced elsewhere in a combined cycle with an efficiency η_{cc}. According to these considerations, two definitions of thermal-to-electrical process efficiency can be computed for this process with a solar power input $\dot{Q}_s = 100$ MW and a predicted time $t_{sun} = 8$ h of solar radiation on a day with $t_d = 24$ h:

(1) The efficiency without savings owing to the CaO that leaves the process in SPURGE, given by

$$\begin{aligned}\eta_1 &= \frac{\dot{W}_{night}\left(t_d - t_{sun}\right) + \dot{W}_{sun} t_{sun}}{\dot{Q}_s t_{sun}} 100\ \% \\ &= \left(2\dot{W}_{night} + \dot{W}_{sun}\right) 1\ \%\ \mathrm{MW}^{-1}.\end{aligned} \tag{6}$$

(2) The efficiency with savings owing to the CaO that leaves the process in SPURGE, given by

$$\begin{aligned}\eta_2 &= \frac{\dot{W}_{night}\left(t_d - t_{sun}\right) + \left(\dot{W}_{sun} + \frac{\eta_{cc}}{\eta_b}\dot{Q}_p\right) t_{sun}}{\dot{Q}_s t_{sun}} 100\ \% \\ &= \left(2\dot{W}_{night} + \dot{W}_{sun} + \frac{\eta_{cc}}{\eta_b}\dot{Q}_p\right) 1\ \%\ \mathrm{MW}^{-1}.\end{aligned} \tag{7}$$

In these definitions, the net electrical power $\dot{W}_{night}$ [MW] produced when no solar radiation is available is given by

$$\dot{W}_{night} = \dot{W}_{MTURB} + \dot{W}_{HTURB} - \dot{W}_{MCOMP} - \dot{W}_{C,car} - \dot{W}_{T,car}, \tag{8}$$

the net electrical power $\dot{W}_{sun}$ [MW] produced when solar radiation is available is given by

$$\begin{aligned}\dot{W}_{sun} = \dot{W}_{MTURB} + \dot{W}_{ST} - \dot{W}_{P1} - \dot{W}_{MCOMP} - \dot{W}_{MCOMD} - \dot{W}_{HCOMP} \\ - \dot{W}_{C,cal} - \dot{W}_{C,car} - \dot{W}_{T,cal} - \dot{W}_{T,car},\end{aligned} \tag{9}$$

and the supply of thermal power $\dot{Q}_p$ [MW] avoided owing to the CaO that leaves the process is given by

$$\begin{aligned}\dot{Q}_p &= \Delta H_{calc}\left(1 - X_{ave}\right) F_0 = \Delta H_{calc}\left(1 - X_{ave}\right) f_p \left(F_0 + F_R\right) \\ &= \Delta H_{calc} \frac{\left(1 - X_r\right)(1-k) f_p}{k f_p + 1 - k}\left(F_0 + F_R\right).\end{aligned} \tag{10}$$

In the previous equations: $\dot{W}_{MTURB}$, $\dot{W}_{ST}$ and $\dot{W}_{HTURB}$ are the electrical power generated by MTURB, ST, and HTURB; $\dot{W}_{P1}$, $\dot{W}_{MCOMP}$, $\dot{W}_{MCOMD}$, and $\dot{W}_{HCOMP}$ are the electrical power consumed by P1, MCOMP, MCOMD, and HCOMP; $\dot{W}_{C,cal}$, $\dot{W}_{C,car}$, $\dot{W}_{T,cal}$, and $\dot{W}_{T,car}$ are the electrical power consumed by coolers and in the transport of solids on the calciner and carbonator sides; and ΔH_{calc} is the reaction enthalpy of $CaCO_3$ calcination. Note that the last equality in (10) implies that the product $\left(1 - X_{ave}\right) f_p$ increases as f_p increases.

When the water separation process in Section 2.2 is also included, the electrical power consumed by the compressors in that process and the thermal power consumed in the final heating step also need to be accounted for. Note that the water separation process is located on the calciner side, thus the power consumption only occurs when solar radiation is available. Hence, in this case, the expression for the efficiency needs to be modified as

$$\begin{aligned}\eta_3 &= \frac{\dot{W}_{night}\left(t_d - t_{sun}\right) + \left(\dot{W}_{sun} - \dot{W}_{sep} + \frac{\eta_{cc}}{\eta_b}\dot{Q}_p\right) t_{sun}}{\left(\dot{Q}_s + \dot{Q}_{sep}\right) t_{sun}} 100\ \% \\ &= \frac{2\dot{W}_{night} + \dot{W}_{sun} - \dot{W}_{sep} + \frac{\eta_{cc}}{\eta_b}\dot{Q}_p}{1 + \frac{\dot{Q}_{sep}}{\dot{Q}_s}} 1\ \%\ \mathrm{MW}^{-1},\end{aligned} \tag{11}$$

where $\dot{W}_{sep}$ [MW] is the sum of electrical power consumed by COMPi, for $i = 1, \ldots, n$, and $\dot{Q}_{sep}$ [MW] is the supply of thermal power needed for QH2O and QCO2. Note that $\eta_3 = \eta_2$ if $\dot{Q}_{sep} = \dot{W}_{sep} = 0$, and $\eta_2 = \eta_1$ if $\dot{Q}_p = 0$.

2.5. Process configurations

As a result of the previous process description, the following three cases are studied in this work: (1) optimization of the carbonator and main turbine outlet pressures without purge or water separation process, which considers the residual conversion of 15 % in the carbonator and CO_2 as fluidizing gas in the calciner; (2) introduction of a varying solids purge split fraction f_p between 0 and 1, which also considers optimal carbonator and main turbine outlet pressures and CO_2 in the calciner; (3) calcination under water vapor is considered for the optimal value of f_p in case (2), assuming that the mass flow rate of water vapor in the solar calciner is equal to the mass flow rate of solids at the calciner inlet as proposed by Rivero et al. [30], and the efficiency penalty associated with the water separation process is also computed.

3. Results and discussion

This section presents the results for the simulation and optimization of the proposed CaL-TCES process for the three cases presented in Section 2.5.

3.1. Optimization of the carbonator and main turbine outlet pressures

After formulating and solving the optimization problem for maximization of the thermal-to-electrical efficiency η_1, the efficiency can be improved from 38.1 %, in the nominal conditions of the original study by Ortiz et al. [7], to 39.2 %. This is achieved by changing the carbonator and main turbine outlet pressures from 3 bar and 1 bar to 1.485 bar and 0.293 bar, respectively. This shows the importance of optimizing the most relevant decision variables, which allows improving the efficiency. Table 1 shows the contributions of power generation and consumption by the unit operations in the CaL-TCES process for the net electrical power $\dot{W}_{sun}$ and $\dot{W}_{night}$ that are obtained for the optimal values of the carbonator and main turbine outlet pressures.

Table 1
Contributions of power generation and consumption (positive for generation, negative for consumption) by the unit operations in the CaL-TCES process in Sections 2.1 and S1 for the net electrical power $\dot{W}_{sun}$ and $\dot{W}_{night}$ obtained for the optimal values of the carbonator and main turbine outlet pressures.

Unit operation	Power (MW)		Unit operation	Power (MW)	
	$\dot{W}_{sun}$	$\dot{W}_{night}$		$\dot{W}_{sun}$	$\dot{W}_{night}$
HCOMP	−0.68	0	C_1	0.00	0
HCOMP1	−0.78	0	C_2	−0.02	0
HCOMP2	−0.77	0	C_2A/C_2B	0.00	0
HCOMP3	−0.76	0	C_3	−0.05	−0.05
HCOMP4	−0.74	0	COND	−0.06	0
HTURB	0	0.32	HCOMPC1	−0.01	0
HTURB1	0	0.30	HCOMPC2	−0.01	0
HTURB2	0	0.27	HCOMPC3	−0.01	0
MCOMD	−0.07	0	HCOMPC4	−0.01	0
MCOMD1	−0.07	0	MCOMDC1	0.00	0
MCOMD2	−0.07	0	MCOMDC2	0.00	0
MCOMP	−4.56	−4.56	MCOMPC1	−0.04	−0.04
MCOMP1	−4.57	−4.57	MCOMPC2	−0.04	−0.04
MCOMP2	−4.57	−4.57	P1	−0.03	0
MTURB	27.72	27.72	S12	−0.51	−0.51
ST	2.76	0	S2	−1.52	0

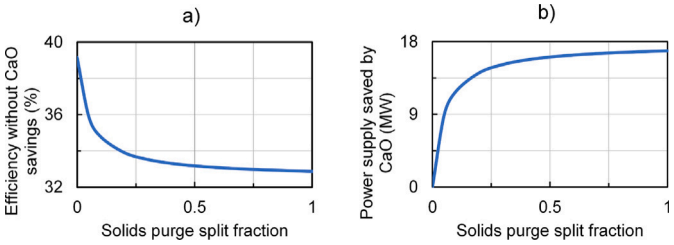

Fig. 7. a) Efficiency η_1 without considering the savings owing to the CaO that leaves the process and b) power supply $\dot{Q}_p$ saved owing to the CaO that leaves the process, both as a function of the solids purge split fraction f_p.

3.2. Effect of the solids purge split fraction

The efficiency η_2 can be improved by increasing the solids purge split fraction f_p from 0 to 1. However, the exact improvement depends on the value of the efficiency ratio $\frac{\eta_{cc}}{\eta_b}$ considered in (7). In this subsection, we assume that the carbonator and main turbine outlet pressures for each value of f_p are the ones that optimize the efficiency η_2 in (7) for $\eta_{cc} = 0.54$ and $\eta_b = 0.90$, which corresponds to $\frac{\eta_{cc}}{\eta_b} = 0.60$. Fig. 7a shows that the efficiency without savings owing to the CaO that leaves the process in SPURGE, which corresponds to η_1 in (6), decreases from 39.2 % to 32.9 % when f_p increases from 0 to 1. This is mainly caused by the reduction in the power generated by MTURB, which decreases from 27.72 MW for f_p equal to 0 to 21.79 MW for f_p equal to 1. On the other hand, Fig. 7b shows that the savings owing to the CaO that leaves the process in SPURGE, which correspond to $\dot{Q}_p$ in (7), increase from 0 % to 16.9 % of the solar input. In both cases, the variation is largest for f_p between 0 and 0.1.

For each efficiency ratio $\frac{\eta_{cc}}{\eta_b}$, the efficiency η_2 with the savings owing to the CaO that leaves the process corresponds to the values in Fig. 7a plus $\frac{\eta_{cc}}{\eta_b}$ times the values in Fig. 7b, which is shown in Fig. 8 for different values of $\frac{\eta_{cc}}{\eta_b}$. The best strategy is to set f_p equal to 1, that is, without a recycle stream between SPURGE and FRESH, if and only if $\frac{\eta_{cc}}{\eta_b}$ is larger than 0.38. For $\frac{\eta_{cc}}{\eta_b} = 0.60$, the efficiency η_2 increases from 39.2 % to 43.0 %. Note that, for other values of $\frac{\eta_{cc}}{\eta_b}$, the carbonator and main turbine outlet pressures and the corresponding efficiency η_2 in Fig. 8 may be slightly suboptimal, and the results in Fig. 8 are shown mainly to illustrate the effect of $\frac{\eta_{cc}}{\eta_b}$ on η_2. To analyze in more detail the factors that affect the savings owing to the CaO, Fig. 9a shows the conversion X_{ave} in the carbonator, which increases from 15.0 %

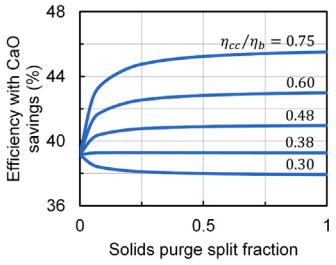

Fig. 8. Efficiency η_2 considering the savings owing to the CaO that leaves the process as a function of the solids purge split fraction f_p for different values of efficiency ratio η_{cc}/η_b.

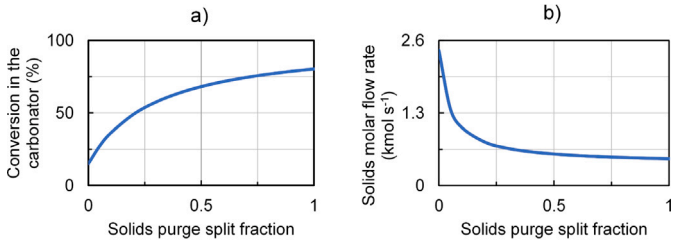

Fig. 9. a) Conversion X_{ave} in the carbonator and b) solids molar flow rate $F_0 + F_R$, both as a function of the solids purge split fraction f_p.

to 80.5 % when f_p increases from 0 to 1 owing to a smaller number of cycles experienced by the particles. Fig. 9b shows the solids molar flow rate F_0+F_R, which decreases for increasing f_p due to a larger fraction of $CaCO_3$ in the solids at the calciner inlet and the fact that all the $CaCO_3$ that enters the calciner needs to be converted to CaO at the expense of the solar power input $\dot{Q}_s$, which is fixed. It can be observed that, although according to (10) both factors contribute to a reduction of $\dot{Q}_p$ for increasing f_p, their effect is not sufficient to overcome the effect of the increase in f_p itself, which explains why $\dot{Q}_p$ ultimately increases as f_p increases. Once again, by considering the existence of make-up and purge streams and the savings in power supply owing to the CaO that leaves the process, it is possible to improve the efficiency.

3.3. Effect of the water separation process

The use of water vapor as a fluidizing gas for the solar calcination reactor affects the residual conversion of the $CaCO_3$/CaO mixture, which can affect the conversion in the carbonator and the efficiency of the whole system. However, as shown by Ortiz et al. [7], the increase of the residual conversion in the carbonator from 10 % to 40 % for the case without purge ($f_p = 0$) only results in an increase of 1.3 % of the overall efficiency, which is significantly smaller than the increase of 3.8 % caused by increasing f_p from 0 to 1 in the current study. In addition, the decreasing effect of the higher residual conversion due to the use of water vapor on the overall efficiency for increasing values of f_p is not sufficient to overcome the increase of the overall efficiency from 39.2 % to 43.0 % when f_p is increased from 0 to 1. This means that, even when water vapor is used as a fluidizing gas, the best option is to use $f_p = 1$. For the best value of f_p equal to 1, the efficiency penalty and several other relevant quantities associated with the water separation process can also be reported. The study about the effect of the water separation process in this section considers the worst-case scenario in which the conversion in the carbonator does not increase if water vapor is used as a fluidizing gas in the solar calcination reactor instead of pure CO_2 when the $CaCO_3$/CaO mixture experiences exactly one cycle in the carbonator. In other words, it is assumed that the conversion in the carbonator for $f_p = 1$, when the $CaCO_3$/CaO mixture

experiences exactly one cycle in the carbonator, is equal to 80.45 % not only if pure CO_2 is used in the solar calcination reactor but also if water vapor is used. Recall that it is assumed that the mass flow rate of water vapor used for fluidization in the solar calciner is equal to the mass flow rate of solids at the calciner inlet. Note that, for $f_p = 1$, the solids at the calciner inlet correspond to pure $CaCO_3$ with a molar flow rate of 0.483 kmol s^{-1}, and at the calciner outlet all the $CaCO_3$ is converted to CaO and CO_2. Hence, the gas outlet of the calciner including water vapor used for fluidization and recycled CO_2 corresponds to a stream with a mass flow rate of 69.6 kg s^{-1} and mass fractions of 0.3055 of CO_2 and 0.6945 of water. The water-rich stream at the outlet of the water separation process corresponds to a mass flow rate of 48.3 kg s^{-1} with a mass fraction of 0.9998 of water, while the CO_2-rich stream at the vapor outlet of the final flash drum FLASH4 corresponds to a mass flow rate of 21.9 kg s^{-1} with a mass fraction of 0.9680 of CO_2. This separation is achieved by specifying the pressures $p_1 = 0.600$ bar, $p_2 = 0.414$ bar, and $p_3 = 0.193$ bar for the separation stages, which correspond to pressure ratios of 1.45 in COMP2 and 2.14 in COMP3 that are determined via optimization.

A heat integration analysis is also performed for the water separation process. It is concluded that 100 % of the heating requirements for the streams in this process that can be heated by another stream are satisfied by the proposed heat integration. Hence, the potential savings for the entire process are fully achieved with the proposed heat exchanger network, and a more detailed heat integration analysis is not necessary for the entire process. This conclusion also supports the proposed use of a modular approach for the separation stages, where heat integration is only performed within each stage. Nevertheless, a detailed heat integration analysis is performed for one of the separation stages in Section S4.

The water separation process implies a consumption of an electrical power $\dot{W}_{sep} = 7.53$ MW (5.08 MW in COMP1, 1.48 MW in COMP2, 0.97 MW in COMP3) and an additional thermal power $\dot{Q}_{sep} = 2.15$ MW (1.74 MW in QH2O, 0.41 MW in QCO2). This means that the thermal-to-electrical efficiency decreases from 43.0 % to 34.7 %, although this reduction may be compensated by the advantages of using water vapor for fluidization in the calciner, such as smaller losses in the receiver or a higher reaction rate and a consequent gain in solar-to-thermal efficiency or a smaller calcination reactor. Hence, there exists a tradeoff between objective (i), the maximization of thermal-to-electrical efficiency, and other important goals, such as objective (ii), the maximization of solar-to-thermal efficiency. This tradeoff between two optimization objectives corresponds to a typical situation of multi-objective optimization, where the set of optimal solutions is described by a Pareto front. In this context, for each level of objective (ii), it is correct to state that the value of objective (i) is optimized, although this value of objective (i) may not be as good as the one that would be achieved if objective (ii) were not considered. More specifically, in this paper, for the level of objective (ii) that corresponds to the use of the water separation process, objective (i) is optimized since the optimal value of $f_p = 1$ and the optimal carbonator and main turbine outlet pressures are used.

Since the use of water vapor for calcination enables a lower temperature in the calcination reactor, the scenario of calcination at 800 °C is also considered in this study of the effect of the water separation process. This analysis shows that the thermal-to-electrical efficiency without inclusion of the water separation process remains equal to 43.0 % when the calcination temperature is decreased from 900 °C to 800 °C, while the efficiency with inclusion of the water separation process is almost unchanged, with a reduction from 34.7 % to 34.4 %. The main changes due to calcination at 800 °C are: a slight reduction of the power generated by MTURB and ST due to the lower temperature of the calcination products, which decreases the efficiency; and an increase in solids molar flow rate at the calciner inlet from 0.483 kmol s^{-1} to 0.500 kmol s^{-1} since less sensible heat is required in the calcination reactor, and a resulting increase in savings owing to the CaO that leaves the process in SPURGE, which increases the efficiency. However, the increase in solids flow rate at the calciner inlet also implies that the gas flow rate at the calciner outlet is larger, which increases the consumption of electrical and thermal power in the water separation process. This means that it remains valid to conclude that the main effects of the use of water vapor for calcination are beneficial and correspond to a gain in solar-to-thermal efficiency or a smaller calcination reactor.

4. Conclusions

This work addresses the simulation and optimization of a calcium-looping process for thermochemical energy storage, with the goal of improving the thermal-to-electrical efficiency. The process includes a solar calciner to transform solar energy into thermochemical energy, a carbonator to release the stored energy, turbines for electrical power generation, storage tanks to store the reaction products before their further use, and heat integration to improve the efficiency. The main novelty lies in: (i) process improvements such as the inclusion of solids make-up and purge streams to increase the conversion in the carbonator and a water separation process at the calciner outlet to allow the use of water vapor as fluidizing gas in the calciner; (ii) process optimization by determining the optimal values of decision variables such as the carbonator and main turbine outlet pressures, solids purge split fraction, and pressure ratios in the water separation process.

By optimizing the carbonator and main turbine outlet pressures, it is possible to improve the efficiency from 38.1 %, as mentioned in the literature, to 39.2 %. When solids make-up and purge streams are considered, and assuming that the ratio between the efficiencies of a combined cycle and of a burner is equal to 0.60, one can conclude that: the efficiency without the savings in power supply for calcination of $CaCO_3$ owing to the CaO in the solids purge decreases from 39.2 % to 32.9 % and the conversion increases from 15.0 % to 80.5 % when the solids purge split fraction increases from 0 to 1; the savings owing to the CaO allow improving the efficiency to 43.0 %; the efficiency with the savings owing to the CaO increases if the combined cycle-burner efficiency ratio is larger than 0.38. If it is not possible to take advantage of the CaO in the solids purge stream, the best option is to have no make-up and purge streams.

A process for separation of the water vapor used as fluidizing gas in a fluidized bed calcination reactor from the CO_2 generated by the calcination reaction is proposed, and the energy consumption required for this process is also accounted for. It is concluded that the thermal-to-electrical efficiency is reduced from 43.0 % to 34.7 % and is almost unchanged when the calcination temperature is decreased from 900 °C to 800 °C, with a further reduction to 34.4 %, although this reduction may be compensated by gains in solar-to-thermal efficiency or a smaller calcination reactor owing to smaller losses in the receiver or smaller residence times.

Future work will consider: (i) the energy consumption required to transport the fresh $CaCO_3$ to the process and the solids purge from the process, which will depend on the location of the concentrating solar power plants with respect to the $CaCO_3$ extraction sites and cement production plants; (ii) the time-varying solar power input throughout the day and the year; (iii) other types of integration between the calcium-looping process and cement production plants, possibly including energy integration; and (iv) other configurations of the CaL-TCES process with integration in combined cycles, as proposed by Ortiz et al. [10].

CRediT authorship contribution statement

D. Rodrigues: Conceptualization, Methodology, Software, Validation, Formal analysis, Investigation, Data curation, Writing – original draft, Writing – review & editing, Visualization. **C.I.C. Pinheiro:** Writing – review & editing, Supervision, Project administration, Funding

acquisition. **R.M. Filipe:** Writing – review & editing, Supervision. **L.F. Mendes:** Writing – review & editing, Supervision. **H.A. Matos:** Writing – review & editing, Supervision, Project administration, Funding acquisition.

Declaration of competing interest

The authors declare that they have no known competing financial interests or personal relationships that could have appeared to influence the work reported in this paper.

Data availability

Data will be made available on request.

Acknowledgments

This work was supported by Fundação para a Ciência e a Tecnologia [grant numbers PTDC/EAM-PEC/32342/2017 for the research project "SoCaLTES - Solar-driven Ca-Looping Process for Thermochemical Energy Storage", UIDB/00100/2020, UIDP/00100/2020 for the research center "Centro de Química Estrutural", UIDB/04028/2020 for the research center "Centro de Recursos Naturais e Ambiente", UIDB/50020/2020, UIDP/50020/2020 for the research center "LSRE-LCM", UIDB/EEA/50009/2020 for the research center "Center for Innovation, Technology and Policy Research (IN+)", LA/P/0056/2020 for the associate laboratory "Institute of Molecular Sciences", and LA/P/0045/2020 for the associate laboratory "ALiCE"].

Appendix A. Supplementary data

Supplementary material related to this article can be found online at https://doi.org/10.1016/j.est.2023.108199.

References

[1] C. Ortiz, J.M. Valverde, R. Chacartegui, L.A. Perez-Maqueda, P. Giménez, The Calcium-Looping (CaCO3/CaO) process for thermochemical energy storage in concentrating solar power plants, Renew. Sustain. Energy Rev. 113 (2019) 109252, http://dx.doi.org/10.1016/j.rser.2019.109252.

[2] R. Chacartegui, A. Alovisio, C. Ortiz, J.M. Valverde, V. Verda, J.A. Becerra, Thermochemical energy storage of concentrated solar power by integration of the calcium looping process and a CO2 power cycle, Appl. Energy 173 (2016) 589–605, http://dx.doi.org/10.1016/j.apenergy.2016.04.053.

[3] Y. Yan, K. Wang, P.T. Clough, E.J. Anthony, Developments in calcium/chemical looping and metal oxide redox cycles for high-temperature thermochemical energy storage: A review, Fuel Process. Technol. 199 (2020) 106280, http://dx.doi.org/10.1016/j.fuproc.2019.106280.

[4] S.E.B. Edwards, V. Materić, Calcium looping in solar power generation plants, Sol. Energy 86 (9) (2012) 2494–2503, http://dx.doi.org/10.1016/j.solener.2012.05.019.

[5] A. Alovisio, R. Chacartegui, C. Ortiz, J.M. Valverde, V. Verda, Optimizing the CSP-Calcium Looping integration for Thermochemical Energy Storage, Energy Convers. Manag. 136 (2017) 85–98, http://dx.doi.org/10.1016/j.enconman.2016.12.093.

[6] C. Ortiz, R. Chacartegui, J.M. Valverde, A. Alovisio, J.A. Becerra, Power cycles integration in concentrated solar power plants with energy storage based on calcium looping, Energy Convers. Manag. 149 (2017) 815–829, http://dx.doi.org/10.1016/j.enconman.2017.03.029.

[7] C. Ortiz, M.C. Romano, J.M. Valverde, M. Binotti, R. Chacartegui, Process integration of Calcium-Looping thermochemical energy storage system in concentrating solar power plants, Energy 155 (2018) 535–551, http://dx.doi.org/10.1016/j.energy.2018.04.180.

[8] S. Pascual, P. Lisbona, M. Bailera, L.M. Romeo, Design and operational performance maps of calcium looping thermochemical energy storage for concentrating solar power plants, Energy 220 (2021) 119715, http://dx.doi.org/10.1016/j.energy.2020.119715.

[9] M. Bailera, S. Pascual, P. Lisbona, L.M. Romeo, Modelling calcium looping at industrial scale for energy storage in concentrating solar power plants, Energy 225 (2021) 120306, http://dx.doi.org/10.1016/j.energy.2021.120306.

[10] C. Ortiz, R. Chacartegui, J.M. Valverde, A. Carro, C. Tejada, J. Valverde, Increasing the solar share in combined cycles through thermochemical energy storage, Energy Convers. Manag. 229 (2021) 113730, http://dx.doi.org/10.1016/j.enconman.2020.113730.

[11] C. Ortiz, C. Tejada, R. Chacartegui, R. Bravo, A. Carro, J.M. Valverde, J. Valverde, Solar combined cycle with high-temperature thermochemical energy storage, Energy Convers. Manag. 241 (2021) 114274, http://dx.doi.org/10.1016/j.enconman.2021.114274.

[12] M. Alvarez Rivero, D. Rodrigues, C.I.C. Pinheiro, J.P. Cardoso, L.F. Mendes, Solid–gas reactors driven by concentrated solar energy with potential application to calcium looping: A comparative review, Renew. Sustain. Energy Rev. 158 (2022) 112048, http://dx.doi.org/10.1016/j.rser.2021.112048.

[13] L. Zhen-shan, C. Ning-sheng, E. Croiset, Process analysis of CO2 capture from flue gas using carbonation/calcination cycles, AIChE J. 54 (7) (2008) 1912–1925, http://dx.doi.org/10.1002/aic.11486.

[14] M. Erans, M. Jeremias, L. Zheng, J.G. Yao, J. Blamey, V. Manovic, P.S. Fennell, E.J. Anthony, Pilot testing of enhanced sorbents for calcium looping with cement production, Appl. Energy 225 (2018) 392–401, http://dx.doi.org/10.1016/j.apenergy.2018.05.039.

[15] D.P. Hanak, E.J. Anthony, V. Manovic, A review of developments in pilot-plant testing and modelling of calcium looping process for CO2 capture from power generation systems, Energy Environ. Sci. 8 (2015) 2199–2249, http://dx.doi.org/10.1039/C5EE01228G.

[16] P. Lisbona, M. Bailera, T. Hills, M. Sceats, L.I. Díez, L.M. Romeo, Energy consumption minimization for a solar lime calciner operating in a concentrated solar power plant for thermal energy storage, Renew. Energy 156 (2020) 1019–1027, http://dx.doi.org/10.1016/j.renene.2020.04.129.

[17] D. Rodrigues, M. Alvarez Rivero, C.I.C. Pinheiro, J.P. Cardoso, L.F. Mendes, Computational model of a Calcium-looping fluidized bed calcination reactor with imposed concentrated solar irradiance, Sol. Energy 258 (2023) 72–87, http://dx.doi.org/10.1016/j.solener.2023.04.018.

[18] Y. Wang, S. Lin, Y. Suzuki, Limestone calcination with CO2 capture (II): Decomposition in CO2/Steam and CO2/N2 atmospheres, Energy Fuels 22 (4) (2008) 2326–2331, http://dx.doi.org/10.1021/ef800039k.

[19] F. Donat, N.H. Florin, E.J. Anthony, P.S. Fennell, Influence of high-temperature steam on the reactivity of CaO sorbent for CO2 capture, Environ. Sci. Technol. 46 (2) (2012) 1262–1269, http://dx.doi.org/10.1021/es202679w.

[20] S. Champagne, D.Y. Lu, A. Macchi, R.T. Symonds, E.J. Anthony, Influence of steam injection during calcination on the reactivity of CaO-based sorbent for carbon capture, Ind. Eng. Chem. Res. 52 (6) (2013) 2241–2246, http://dx.doi.org/10.1021/ie3012787.

[21] V. Manovic, P.S. Fennell, M.J. Al-Jeboori, E.J. Anthony, Steam-enhanced calcium looping cycles with calcium aluminate pellets doped with bromides, Ind. Eng. Chem. Res. 52 (23) (2013) 7677–7683, http://dx.doi.org/10.1021/ie400197w.

[22] S. Guo, H. Wang, D. Liu, L. Yang, X. Wei, S. Wu, Understanding the impacts of impurities and water vapor on limestone calcination in a laboratory-scale fluidized bed, Energy Fuels 29 (11) (2015) 7572–7583, http://dx.doi.org/10.1021/acs.energyfuels.5b01218.

[23] J. Arcenegui-Troya, P.E. Sánchez-Jiménez, A. Perejón, V. Moreno, J.M. Valverde, L.A. Pérez-Maqueda, Kinetics and cyclability of limestone (CaCO3) in presence of steam during calcination in the CaL scheme for thermochemical energy storage, Chem. Eng. J. 417 (2021) 129194, http://dx.doi.org/10.1016/j.cej.2021.129194.

[24] J.J. Arcenegui Troya, V. Moreno, P.E. Sanchez-Jiménez, A. Perejón, J.M. Valverde, L.A. Pérez-Maqueda, Effect of steam injection during carbonation on the multicyclic performance of limestone (CaCO3) under different calcium looping conditions: A comparative study, ACS Sustain. Chem. Eng. 10 (2) (2022) 850–859, http://dx.doi.org/10.1021/acssuschemeng.1c06314.

[25] J. Arcenegui-Troya, P.E. Sánchez-Jiménez, A. Perejón, J.M. Valverde, L.A. Pérez-Maqueda, Steam-enhanced calcium-looping performance of limestone for thermochemical energy storage: The role of particle size, J. Energy Storage 51 (2022) 104305, http://dx.doi.org/10.1016/j.est.2022.104305.

[26] T. Tone, M. Hotta, N. Koga, Acceleration effect of atmospheric water vapor on the thermal decomposition of calcium carbonate: A comparison of various resources and kinetic parameterizations, ACS Sustain. Chem. Eng. 10 (34) (2022) 11273–11286, http://dx.doi.org/10.1021/acssuschemeng.2c03062.

[27] Y. Fang, Y. Li, Y. Dou, Z. He, J. Zhao, Effect of steam on heat storage and attrition performance of limestone under fluidization during CaO/CaCO3 heat storage cycles, React. Chem. Eng. 7 (2022) 2093–2106, http://dx.doi.org/10.1039/D2RE00164K.

[28] J.C. Abanades, E.J. Anthony, J. Wang, J.E. Oakey, Fluidized bed combustion systems integrating CO2 capture with CaO, Environ. Sci. Technol. 39 (8) (2005) 2861–2866, http://dx.doi.org/10.1021/es0496221.

[29] M.C. Romano, Modeling the carbonator of a Ca-looping process for CO2 capture from power plant flue gas, Chem. Eng. Sci. 69 (1) (2012) 257–269, http://dx.doi.org/10.1016/j.ces.2011.10.041.

[30] M.A. Rivero, D. Rodrigues, C.I.C. Pinheiro, J.P. Cardoso, L.F. Mendes, Modelling a calcium-looping fluidised bed calcination reactor with solar-driven heat flux, Chem. Eng. Trans. 88 (2021) 871–876, http://dx.doi.org/10.3303/CET2188145.